TECHNICAL REPORT No. 24

ON THE AVERAGE ERRORS OF AN ENSEMBLE OF FORECASTS

by

J. Derome

February 1981

This work was done while the author was on sabbatical leave from McGill University, Montreal, Canada.

C O N T E N T S

ABSTRACT

The average error fields of an ensemble of 10-day forecasts made with a global model at the European Centre for Medium Range Weather Forecasts and first presented by Hollingsworth et al (1980) are examined. The time evolution of the error fields is presented together with horizontal and vertical cross-sections through the fields at fixed times to reveal some features of their three-dimensional structures. The most striking deficiency of the model is seen to be its inability to maintain the amplitude of the quasi-stationary zonal wave number 2 in the middle and upper troposphere.

1. INTRODUCTION

Hollingsworth et al (1980) have described the results of seven forecasts made with a global model at the European Centre for Medium Range Weather Forecasts (ECMWF). They commented on the relatively important part of the forecast errors associated with the "systematic" or "average" errors and suggested that they be examined in more detail. The present study attempts to do this in an effort to better document the structure and time evolution of the average error fields.

It is realized that the sample of seven cases used in this study is small. On the other hand, as this work was being initiated, more information was gradually becoming available on the systematic errors of the ECMWF model run on an operational basis, which showed that indeed the seven cases discussed by Hollingsworth et al had average errors which were quite representative, in terms of geographical distribution, of those obtained with more cases. It was thus decided to continue the analysis of the seven cases which is reported here.

2. THE FORECAST MODEL AND DATA

Since the main characteristics of the forecast model used in these experiments have already been presented by Hollingsworth et al, only a very brief summary will be given here. The model is global, uses an enstrophy conserving finite difference scheme with a zonal and meridional resolution of 1.875 degrees. It has 15 levels in the vertical, from $\sigma = 0.025$ to 0.996 where σ is the pressure divided by the surface pressure. The sub-grid scale parameterization was that described by Tiedtke et al (1979) and denoted by "EC" by Hollingsworth et al. It includes the following processes: (1) radiative exchanges with model-predicted humidity and cloud fields, (2) surface fluxes and turbulent vertical fluxes of momentum, sensible heat and moisture, (3) condensation due to large-scale processes and convection, (4) prediction of soil moisture and snow amount.

The initial data for the forecasts were the NMC Washington analyses for February 3, 6, 9, 12, 15, 18 and 22, 1976, supplemented with 10 mb analyses for the Northern Hemisphere from the United Kingdom Meteorological Office and 10 mb climatological data for the Southern Hemisphere.

The average of the seven forecasts and of the corresponding analyzed fields at 12 hour intervals from t = 0 to t = 10 days were made available to the author. More precisely, the variables made available were the Fourier sine and cosine coefficients of the height field and of the zonal and meridional components of the wind up to zonal harmonic m = 20, from north pole to south pole at intervals of 1.875 degrees of latitude, and at pressure levels p = 50, 100, 150, 200, 250, 300, 400, 500, 700, 850, 1000 mb.

3. THE AVERAGE ERRORS

3.1 500 and 1000 mb maps

The ensemble average of the seven height forecasts at t = 10 days is compared in Fig. 1 to the corresponding ensemble average of the verifying analyses at both 500 mb and 1000 mb. These maps have already been presented by Hollingsworth et al but they are reproduced here for convenience. Some of the deficiencies of the model are quite evident. For example, at 500 mb the analyses show a ridge over the Greenwich meridian from about 40° N to the pole, whereas the model has, on the average, a trough. Similarly, the model heights are too low in the Gulf of Alaska, which leads to excessively strong height gradients over the northeastern Pacific. The reverse is observed over eastern North America where the model height gradients are rather weak compared to the observed ones. Similar comments apply to the 1000 mb heights in the sense that the predicted heights are much too low along 0° W north of 40° N and over the Gulf of Alaska. The meridional height gradient over North America, from about 40° N to 60° N, is seen to be clearly too strong in the ensemble average of the forecasts.

To give a better appreciation of the average error of the forecasts and of its time evolution we present in Fig. 2 the average difference field, i.e., forecast minus analyzed, at 500 mb for t = 2, 6 and 10 days. We see that the dominant error patterns at t = 10 days, for example, the low heights along 0° E, 90° E and 160° W were already well established at t = 6 days and indeed they are easily discernible even at t = 2 days. The maximum errors are relatively far north, around 55° N; because of the geostrophic nature of the flow, however, the maximum error in the stream function might be expected to occur at lower latitudes.

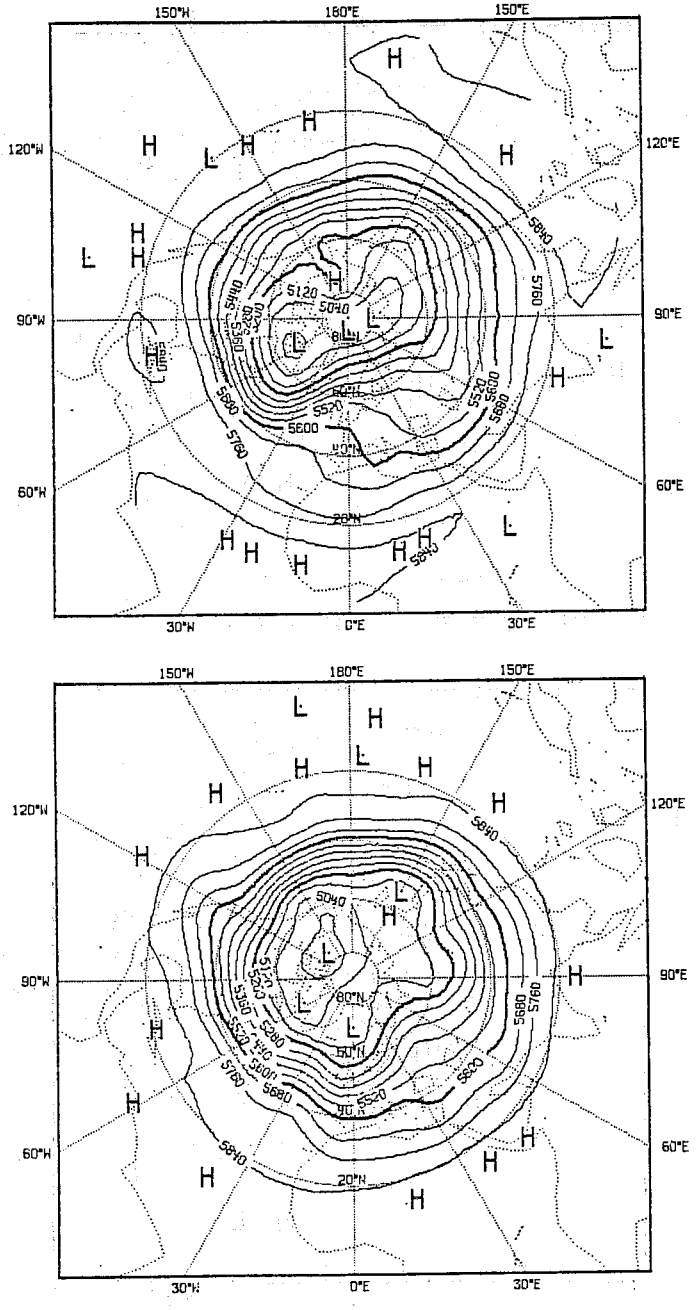

Fig. 1 (a) Ensemble mean of analyzed height fields at t = 10 days, 500 mb; 80 m contour intervals. (b) Same as (a) but for the forecasts.

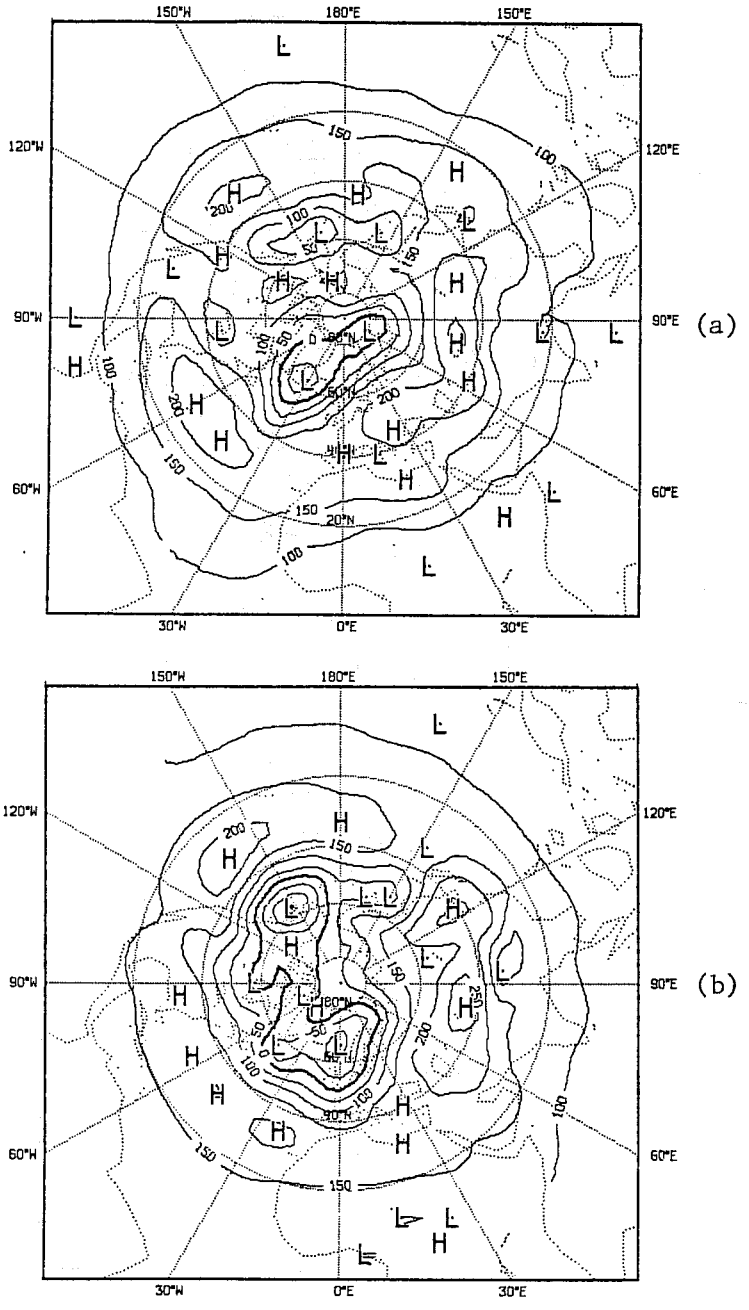

Fig. 1 (c) Ensemble mean of analyzed height fields at t = 10 days, 1000 mb; 50 m contour intervals. (d) Same as (c) but for the forecasts.

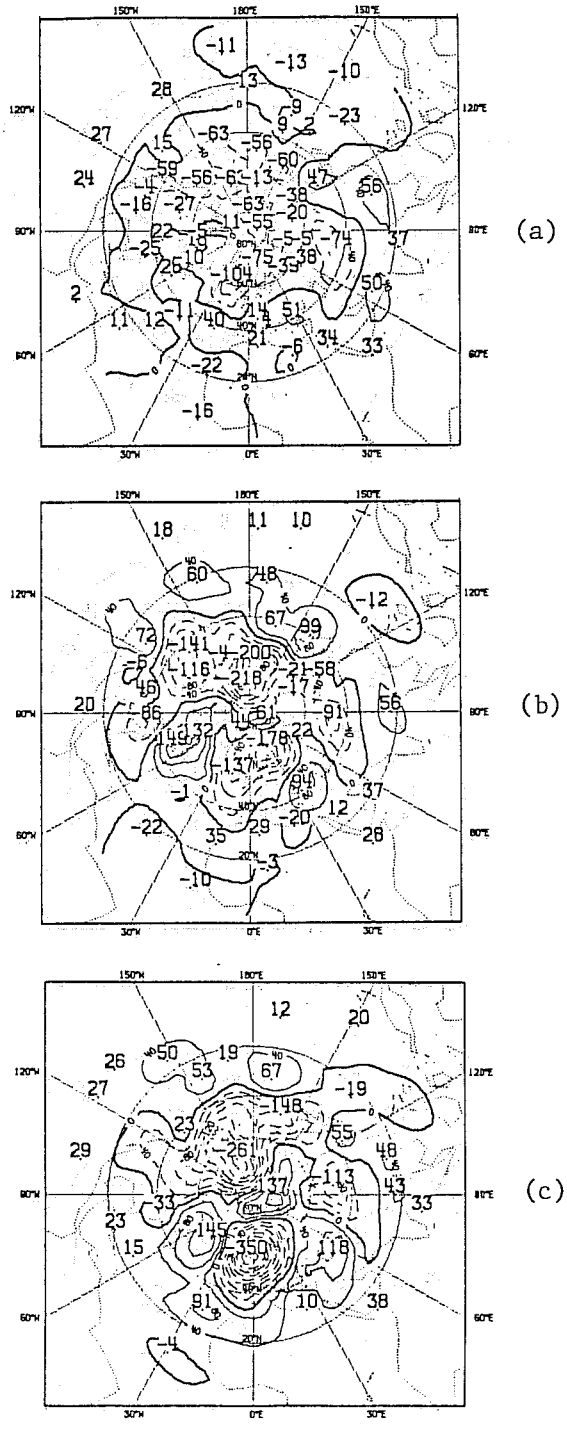

Fig. 2 Ensemble mean of 500 mb forecast errors at: (a) t = 2 days, (b) t = 6 days and (c) t = 10 days. The contour interval is 40 m; the zero contours are thicker and negative contours are dashed.

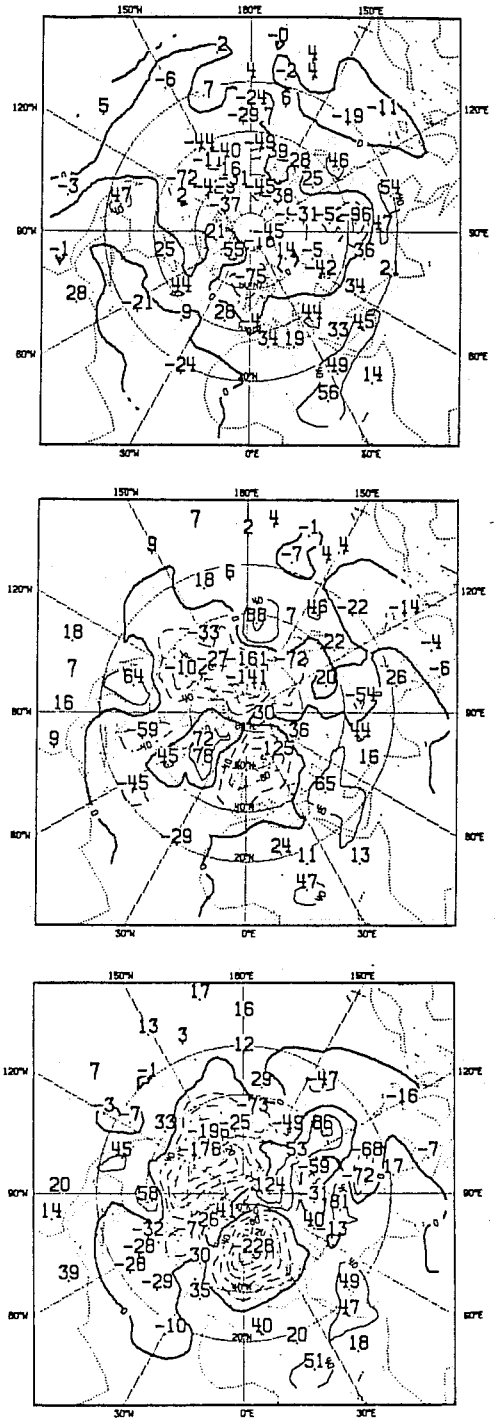

Fig. 3 As in Fig. 2 but at 1000 mb.

Fig. 3 gives the forecast error maps at 1000 mb for the same times as Fig. 2, namely, t = 2, 6 and 10 days. By comparing Figs. 2 and 3 we observe the same general features. For example, the large negative values over the Gulf of Alaska and the northeastern Atlantic - western Europe are present both at 1000 mb and 500 mb, although with less intensity at the lower level, implying a temperature error in the layer approximately in phase with the height error. We will present a vertical cross-section of the temperature error in the sequel.

3.2 Examination of possible meridional error propagation

It seems then, from Fig. 3 that there is relatively little meridional propagation of the average error. Because the variance in the height field is much lower in the tropics and subtropics than in the middle and high latitudes, both in the forecasts and in the analyses, it may be argued that the geopotential height is not the most natural variable to look at if we are interested in meridional propagation. Hoskins and Karoly (1980), for example, have shown that a steady source of wave energy in the tropics can lead to a steady disturbance in the geopotential which has a maximum amplitude in the northern latitudes while being quite weak in the source region. To see whether the average error of the model in the northern latitudes might be due to an improper specification of the quasi-stationary wave energy sources in the tropics it was therefore decided to examine the average error in the wind field.

The ensemble mean vector wind error was first averaged, in a rms sense, over longitude at each latitude and pressure level where data were available. The computations were done at 12-hour intervals from t = 0 to t = 10 days and the results were smoothed in time by means of a filter with weights 0.25, 0.50, 0.25 to remove a diurnal oscillation associated with the analyses of zonal wave number one. Finally, the error was averaged in the vertical, leaving a field which is a function of latitude and time. The result appears in Fig. 4. We see that at least during the first few days, the wind error grows at all latitudes. In the tropical latitudes the error reaches a quasi-equilibrium after about four days whereas in the middle and high latitudes the growth continues over most of the forecast period. In general, there seems to be no evidence of a significant propagation of the error over wide latitude bands. In view of this we will focus our attention on the height forecast error at a fixed latitude, namely 56^{o} N, where the error is particularly large (see Fig. 2).

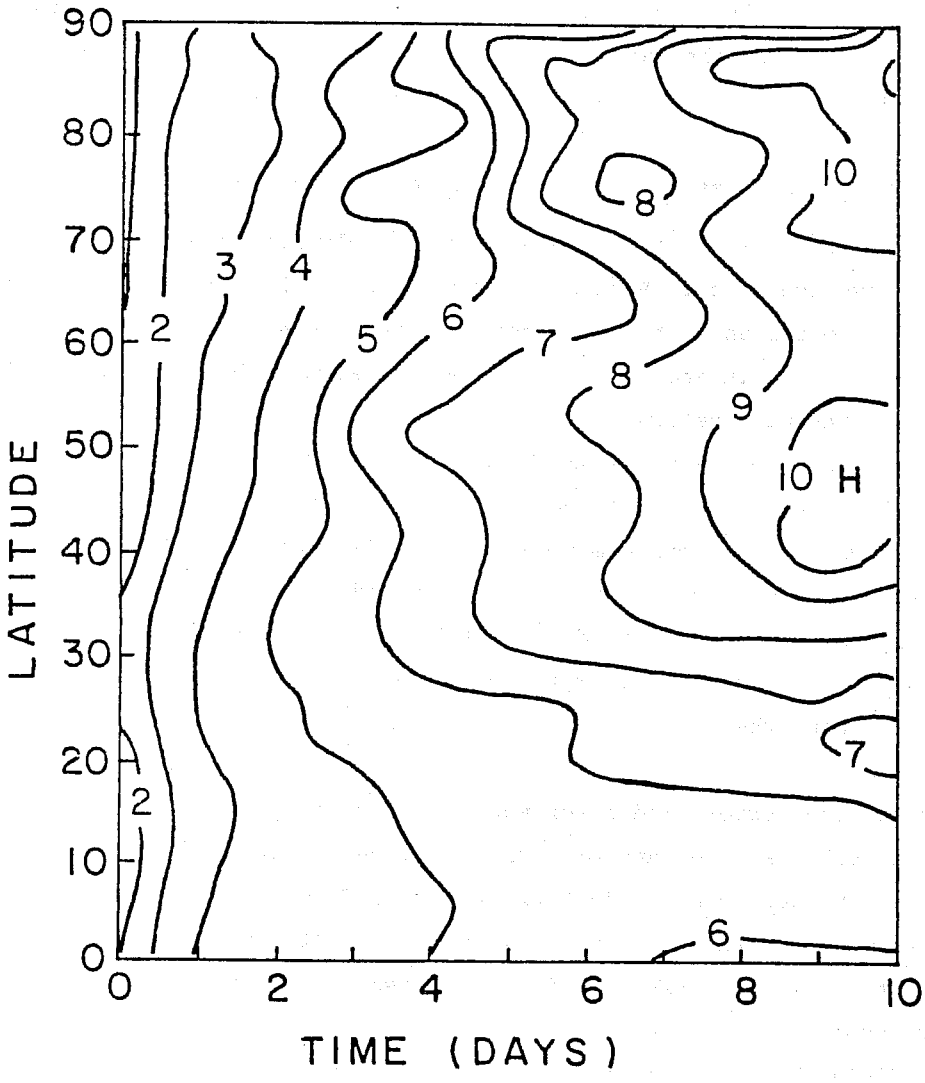

Fig. 4 Vertical average of the rms wind forecast error along latitude circles, as function of latitude and time. The contour interval is 1 m s^{-1}.

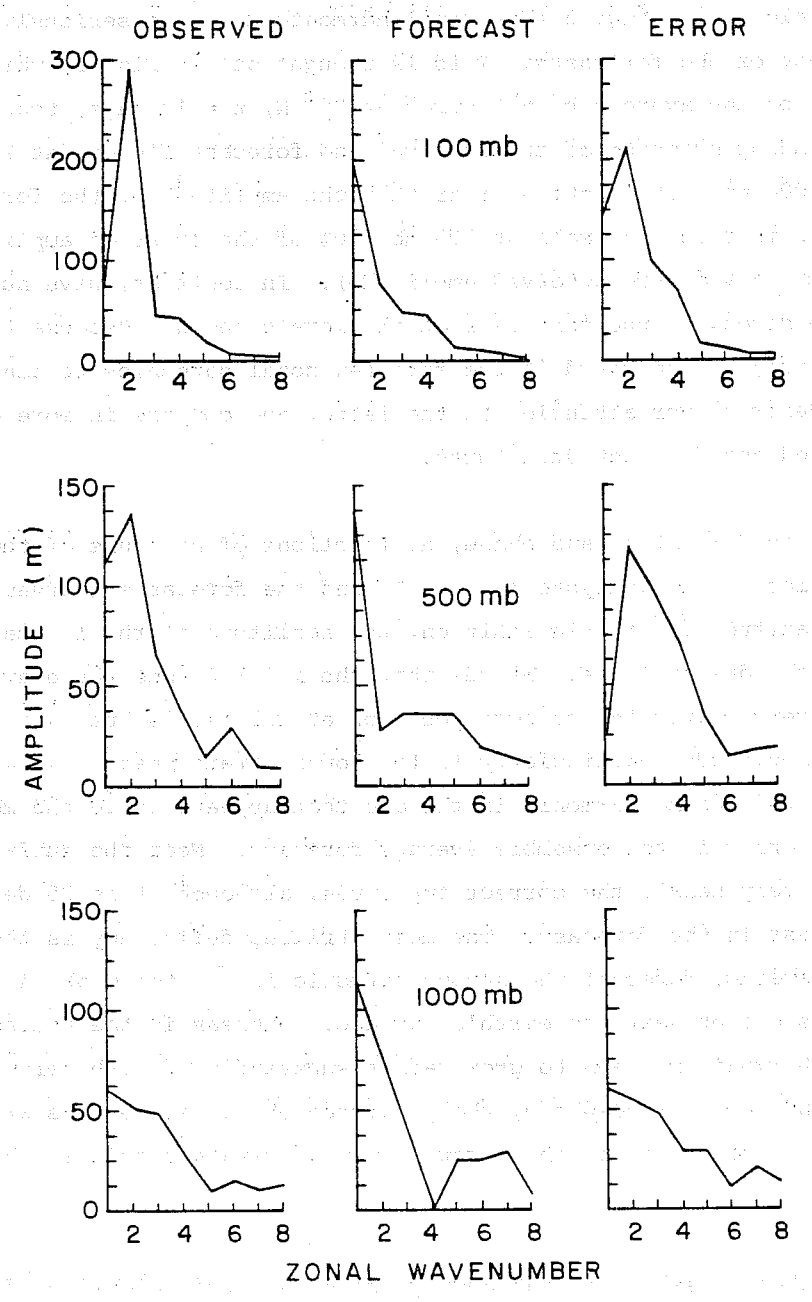

Fig. 5 Amplitudes of zonal wave numbers 1 to 8 at 56° N in the ensemble means of the height analyses (left), height forecasts (centre) and height forecast errors (right) at 100 mb, 500 mb and 1000 mb.

3.3 Spectrum of the height error

It is quite clear from Fig. 2 that zonal harmonic m = 2 is seriously in error in the average of the forecasts. This is brought out in Fig. 5, which gives the spectrum of the average height error at 56° N, t = 10 days, together with the corresponding spectrum of the observed and forecast fields, at 100 mb, 500 mb and 1000 mb. It is quite clear that the amplitude of the forecast wave number 2 is much too small at 500 mb (20% of the observed amplitude) and at 100 mb (26% of the observed amplitude). In contrast, wave number 1 is somewhat too strong in the forecasts at all levels shown. Because the forecast error is clearly concentrated in the firt few zonal harmonics we can, for the moment, concentrate our attention on the latter and compare in more detail their observed and forecast structures.

Fig. 6 gives the amplitude and phase, as functions of pressure of the first three harmonics in the analyses (curves A) and the forecasts (curves F) at day 10 and latitude 56° N; in addition, the amplitude of the forecast error is given by the dashed lines. We see that the model places the gravest harmonic in very nearly the correct position at all levels but that it gives it too much amplitude, particularly in the lower stratosphere. As we have seen before, the second harmonic is the one that appears to be the most seriously in error in the ensemble average forecast. Near the surface this harmonic has very nearly the correct amplitude, although it is 25 degrees too far to the east in the forecast. The most striking deficiency is the fact that in the average forecast the second harmonic is far too weak in amplitude at all levels except near the earth's surface. Whereas in the average analysis the average harmonic is seen to grow rather substantially with height throughout the middle and upper troposphere, the predicted one first weakens with height in the lower troposphere and then grows somewhat with altitude in the upper troposphere.

Another remarkable feature of the average forecast error highlighted by Fig. 6 is its strong (equivalent) barotropic component. For example, we see in the centre panel of Fig. 6b that the phase of the error harmonic number 2 changes by less than 16 degrees at all levels in the vertical. Similarly, the third harmonic in the error is very nearly vertical. This does not imply, on the other hand, that the forecast and analyzed harmonics bear a constant phase relationship with each other throughout the depth of the atmosphere. The forecast harmonic number 2, for example, is to the east of the analyzed one in the lower and middle troposphere but it is exactly in phase with it at 200 mb. (The fact that the phase of the error is 90 degrees, or half a wavelength, out of phase with the analyzed and forecast waves is simply a

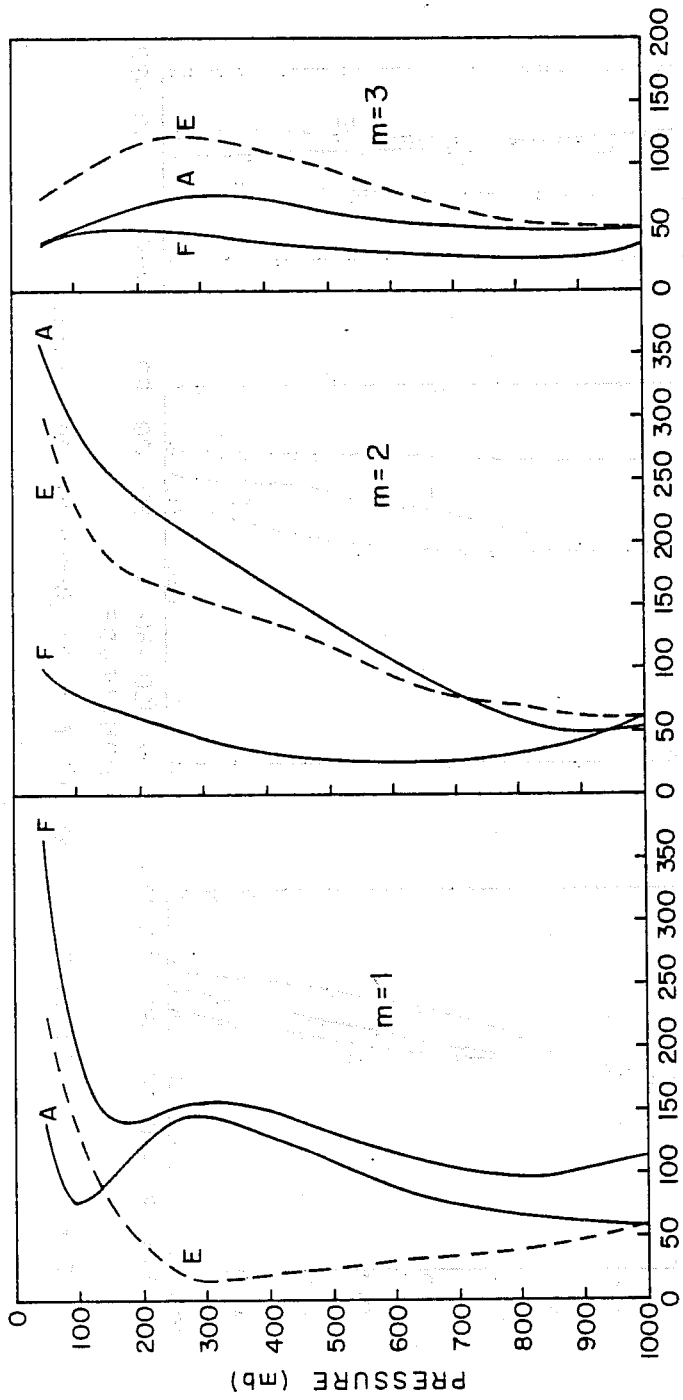

Fig. 6(a) Amplitude in metres as a function of pressure for the ensemble mean of the forecasts (curves F), analyses (curves A) and forecast errors (curves E) for zonal wave numbers 1, 2 and 3 at 56° N.

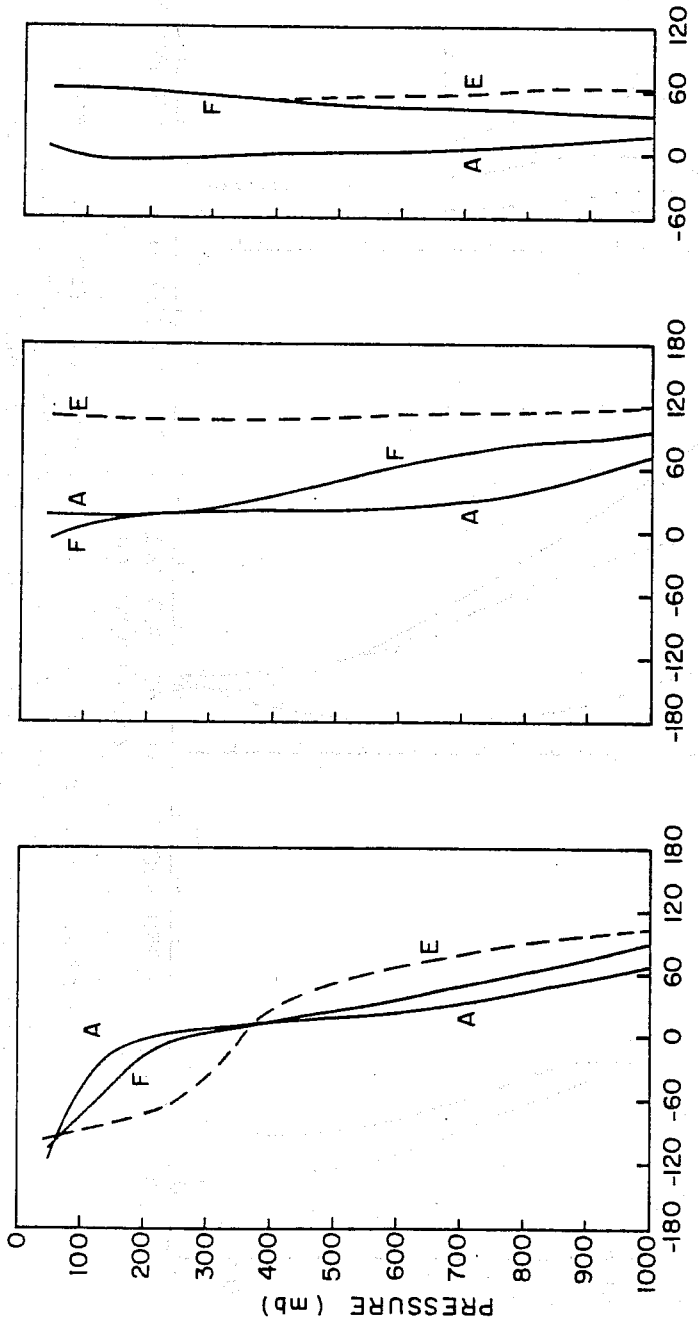

Fig. 6(b) As in Fig. 6(a) but for the phase of the waves.

manifestation of the fact that the difference between two sinusoids that are in phase with each other is also a sinusoid which is either exactly in phase or exactly half a wavelength out of phase with the original ones).

As for the third harmonic, we find that it is too weak and much too far to the east in the predictions. In the upper troposphere, for example, the forecast and analyzed harmonics are approximately 60 degrees, or half a wavelength out of phase.

Having stressed the equivalent barotropic nature of the error harmonics 2 and 3, we should not lose sight of the fact that the error in the first harmonic is quite different. The latter, in fact, slopes to the west by 204 degrees from 1000 to 50 mb, that is, by more than half a wavelength. Of course, when all the harmonics are added to produce the error map, the second and third harmonics dominate the first in amplitude, at least in the troposphere, with the net result that the error patterns look very nearly vertical (see Figs. 2(c) and 3(c)).

The time evolution of the average error spectrum can be seen in Figs. 7 and 8 for the 500 and 1000 mb levels, respectively. The lower part of the figures gives the error amplitude in metres for the first five zonal harmonics at $t = 2$, 6 and 10 days, while the upper part of the figures present the corresponding normalized amplitudes, that is, the error amplitude divided by the amplitude in the average analyses. We see that at 500 mb, the error spectrum in the early stages of the forecast (two days) is relatively flat but as time progresses the dominance of the longer waves becomes manifest. In terms of the normalized error, however, the spectrum is quite different. We see there that with time the shorter waves dominate. In other words, the large error found, for example, in zonal wave number 2 in the forecasts is a reflection of the fact that the observed mean atmospheric state has a large variance on that scale, rather than some model deficiency which is peculiar to that scale.

At 1000 mb (Fig. 8) the time evolution of the error is somewhat more complex, but again we see that in the initial stages of the forecasts (two days) the amplitude of the average error is nearly uniform over the scales shown but in time the larger scales become dominant. In terms of the normalized error, however, we find that the larger scales are not predicted worse than the shorter ones.

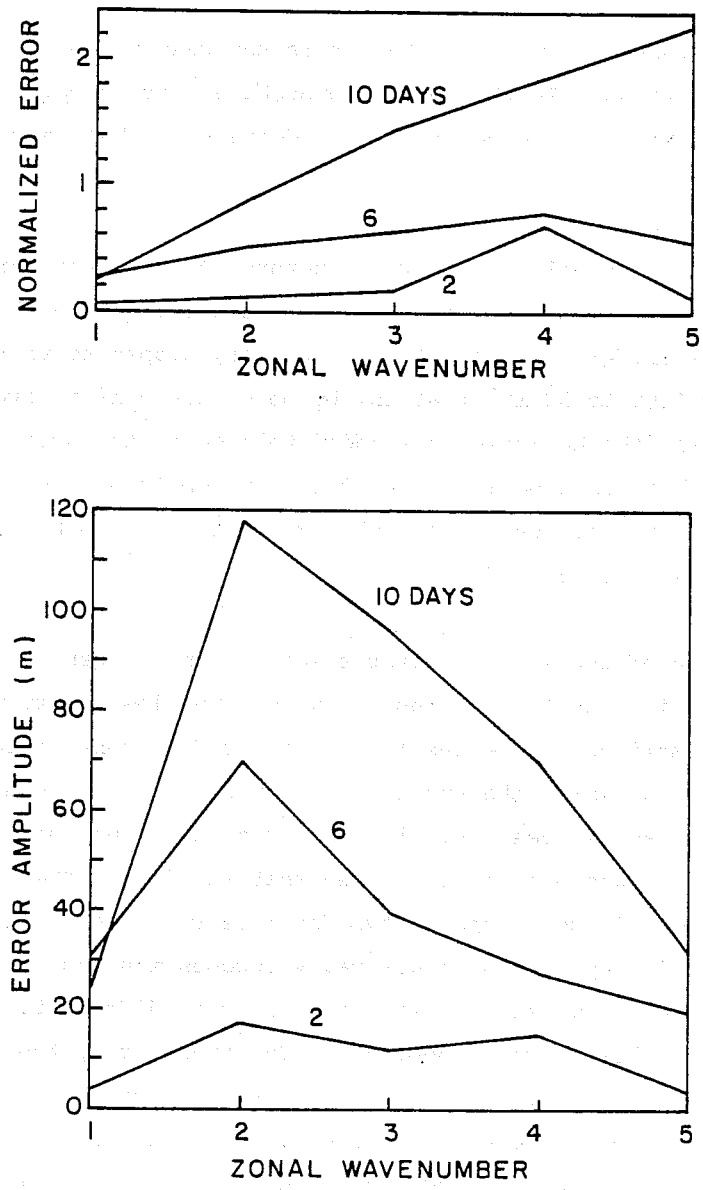

Fig. 7 Bottom: amplitude in metres of the forecast error as a function of zonal wave number at t = 2, 6 and 10 days at 500 mb, 56° N. Top: as at bottom but for the normalized error, that is, the error amplitude divided by the observed amplitude.

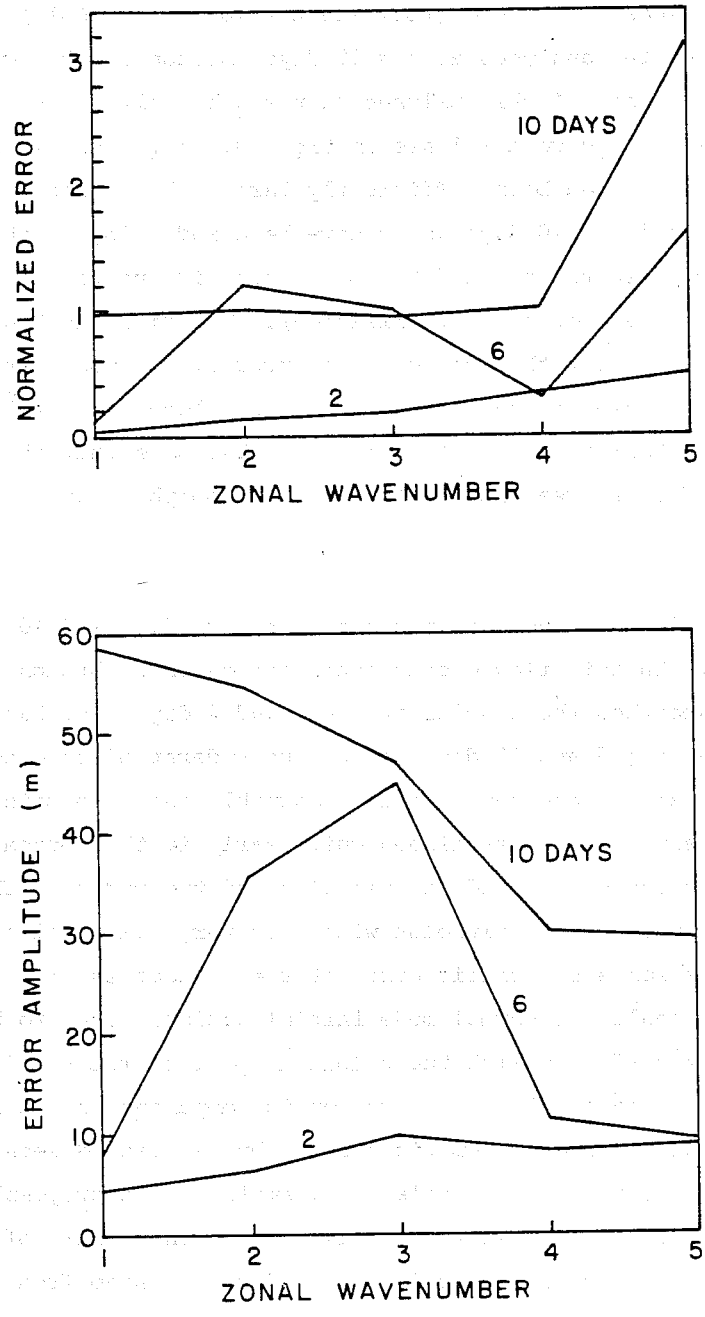

Fig. 8 As in Fig. 7 but at 1000 mb.

3.4 Vertical structure

To help visualize the vertical structure of the average height error, vertical cross-sections along 56° N were prepared. We present first in Fig. 9, the average of the forecasts at t = 0 (top) and t = 10 days (middle) together with the average of the analyses at t = 10 days (bottom). The top figure differs from the average of the analyses at t = 0 by only the effect of the initialization, which, as we shall see in Fig. 10, is relatively small. If our number of cases had been sufficiently large, the average of the analyses at t = 0 and t = 10 days would have been indistinguishable. The difference then between the top and bottom figures id due to our small sample size (plus the small effect of initialization). By comparing the middle and bottom figures we see that the most evident error of the model at t = 10 days is its inability to maintain the low centre which slopes from 40° W at the surface (Icelandic Low) to 70° W at 50 mb. We also note that the model shifts the ridge centered over Greenwich in the upper troposphere much too far to the east.

Similar cross-sections of the height error at t = 0, 2, 6 and 10 days are shown in Fig. 10. In this figure only zonal harmonics 1 through 4 were retained; this smoothed the results at t = 0 and 2 days, but had very little effect on those at t = 6 and 10 days, as can be understood from our previous discussion of the error spectrum. It is remarkable that the main features of the error pattern become established quite early in the forecast period. In fact, the low heights centered at Greenwich and the ridge to the west of it can be seen even at t = 0, although with only very weak amplitude. The most obvious cause for a systematic error at t = 0, that is, for a systematic effect due to the nonlinear normal mode initialization, seems to be the fact that the latter is performed with the adiabatic part of the model only. As the diabatic heating certainly has a systematic component, there is no doubt that its neglect can have a systematic effect, but as can be seen in Fig. 10, top panel, the effect seems to be relatively small in the troposphere. The larger values in the lower stratosphere may well be the result of the fact that the analyses there were produced by a different system from those in the troposphere. It is not suggested here that the average errors found in the forecasts is caused by errors in the initial conditions of the model. In fact, there seems to be evidence to the contrary. For example, Arpe (1980) has described the results of a 50-day integration of the model and has shown that when the model states are averaged over days 24 to 48, the resulting model climatology differs from the atmospheric climatology in a manner which is quite reminiscent of the average errors described in the present study. It would appear then that the average errors of the model are not primarily due to poorly specified initial conditions but rather to a model deficiency.

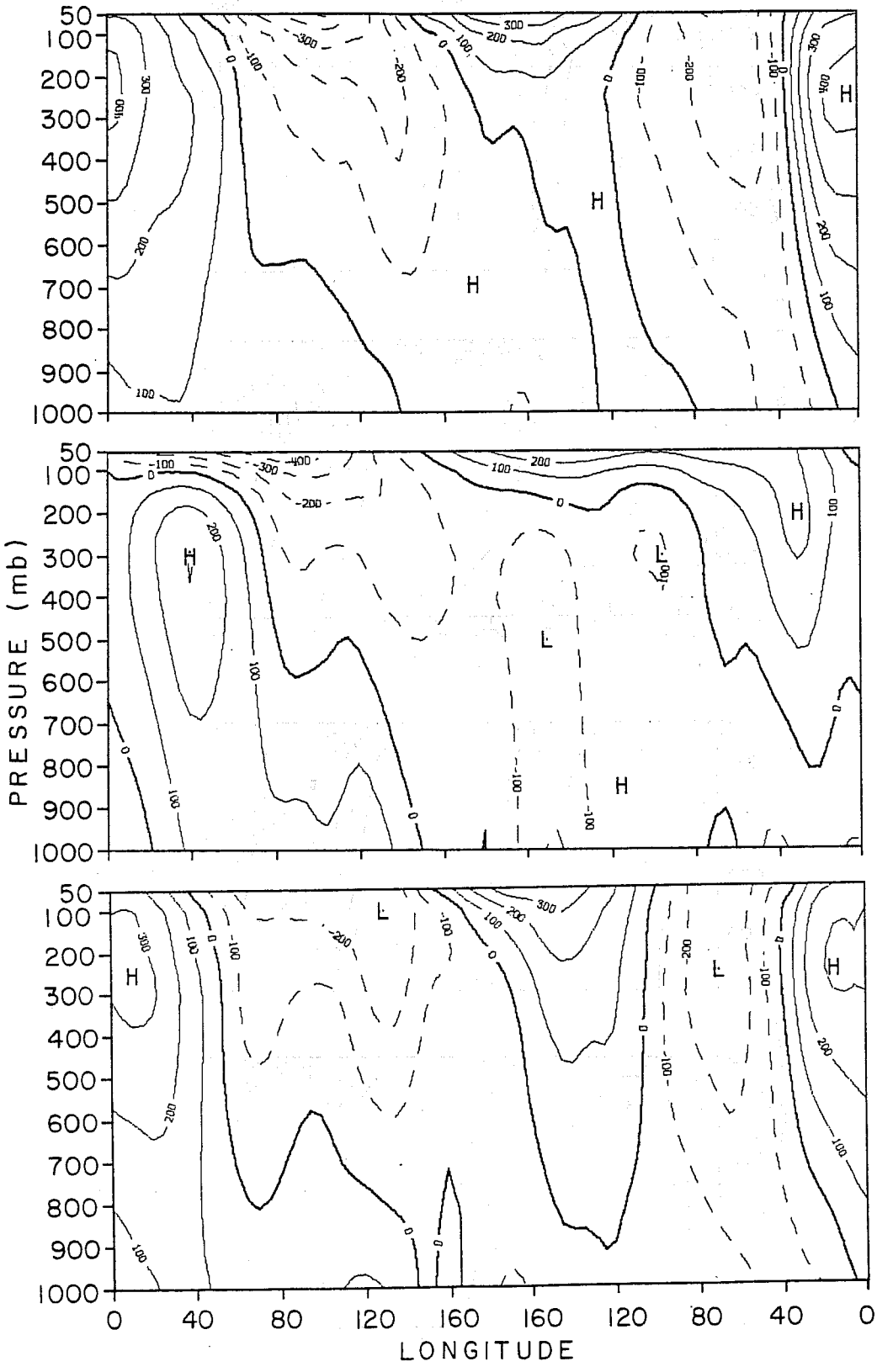

Fig. 9 Ensemble mean height field as a function of pressure and longitude at 56°N, as a deviation from the zonal average. Top: mean of forecasts at t = 0. Centre: mean of forecasts at t = 10 days. Bottom: mean of analyses at t = 10 days. The contour interval is 100 m and the dashed contours are negative.

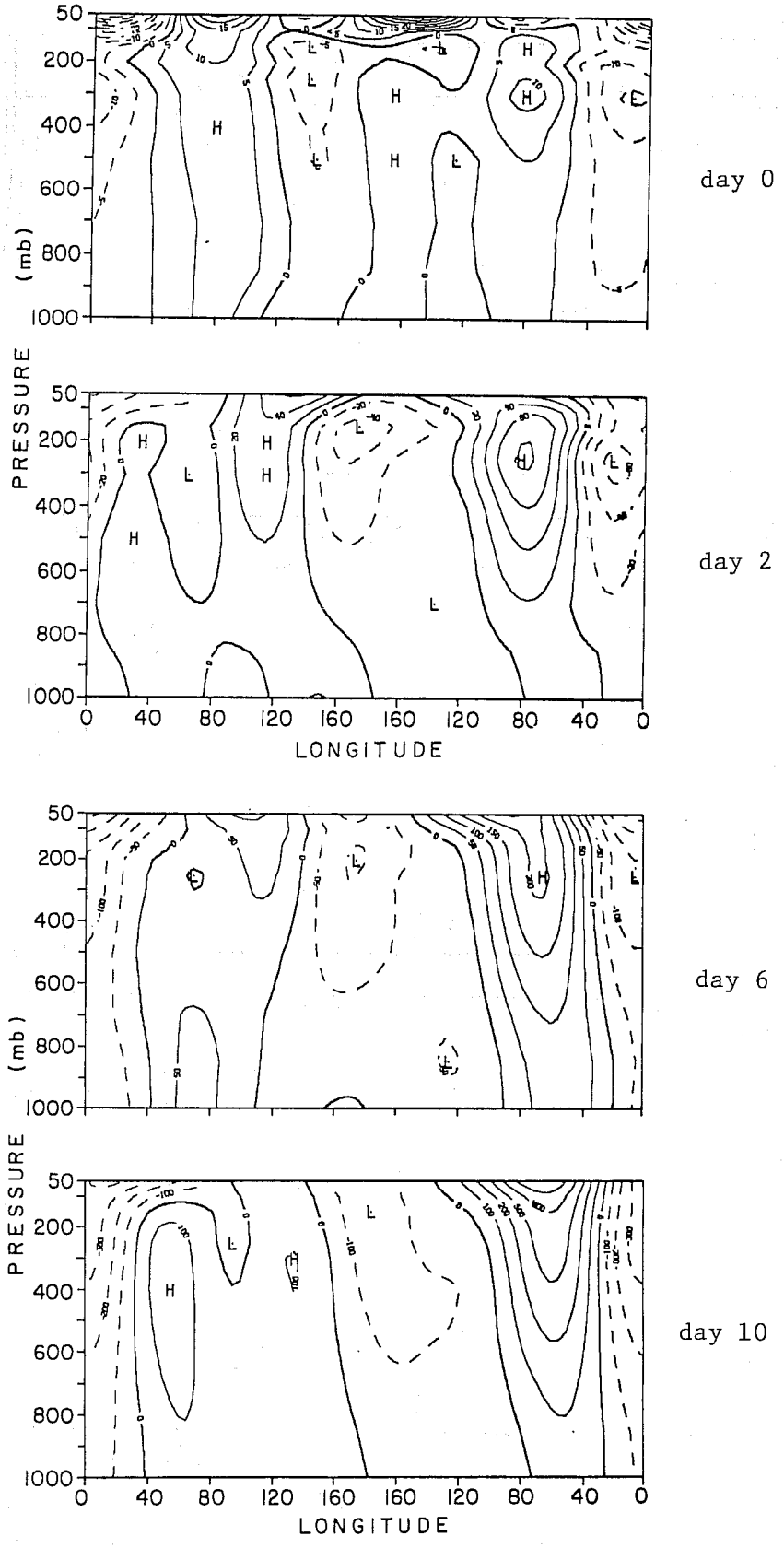

Fig. 10 Ensemble mean of the height forecast error as a function of pressure and longitude at 56^{o}N as a deviation from the zonal mean. (a) t = 0, contour interval 10 m; (b) t = 2 days, contour interval 20 m; (c) t = 6 days, contour interval 50 m; (d) t = 10 days, contour interval 100 m.

The temperature error at t = 10 days (associated with the bottom part of Fig. 10) is shown in Fig. 11. We see that the average forecast is as much as 10^{o} C too warm along the east coast of Canada in the middle troposphere and 8^{o} C too cold near the Greenwich meridian. In general, the temperature error patterns are deep, extending from the ground to the tropopause; in the lower stratosphere, separate error patterns are observed, with amplitudes comparable to those of the troposphere. In short, the temperature errors are large at t = 10 days and while the geopotential height error patterns do not slope very much with height, they are not truly barotropic but rather nearly "equivalent barotropic".

3.5 East-west displacements

The zonal displacement of the error in time can be visualized by means of Hovemoller diagrams, or time-longitude plots. In Figs. 12, 13 and 14, we present such diagrams for the 100, 500 and 1000 mb levels, respectively. In each figure, the top panel applies to the average analysis, the middle one to the average forecast and the bottom one to the average error.

We note first that for a sufficiently large number of analyses, the lines in the top panels would be vertical. In general, our sample seems reasonable in that the analyses change relatively little from day to day, but is is clear that there are some oscillations and these will have to be borne in mind in the interpretation of the time behaviour of the error. It should be clear that time changes in the error field on the time scale of the oscillations seen in the top panels of Figs. 12, 13 and 14 may well be due to sample deficiencies and should not be interpreted as representative of the systematic error of the model. Fortunately the bulk of the average error, as can be seen in the bottom panels is associated with a rather long time scale growth and motion which should be more representative of the systematic errors of the model than the higher frequency changes.

Referring to the middle panels of Figs. 12, 13, 14 we see very clearly the tendency of the model to fill the low pressure area near 60^{o} W, particularly at 500 and 100 mb where, in fact, the model eventually builds a ridge. The fact that the upper levels are more strongly affected than the lower levels is simply indicative of the fact that the troposphere is gradually warming in that region in the model, as was seen in Fig. 11. The other striking error of the model is its tendency to shift the European ridge eastward, particularly in the middle and lower troposphere.

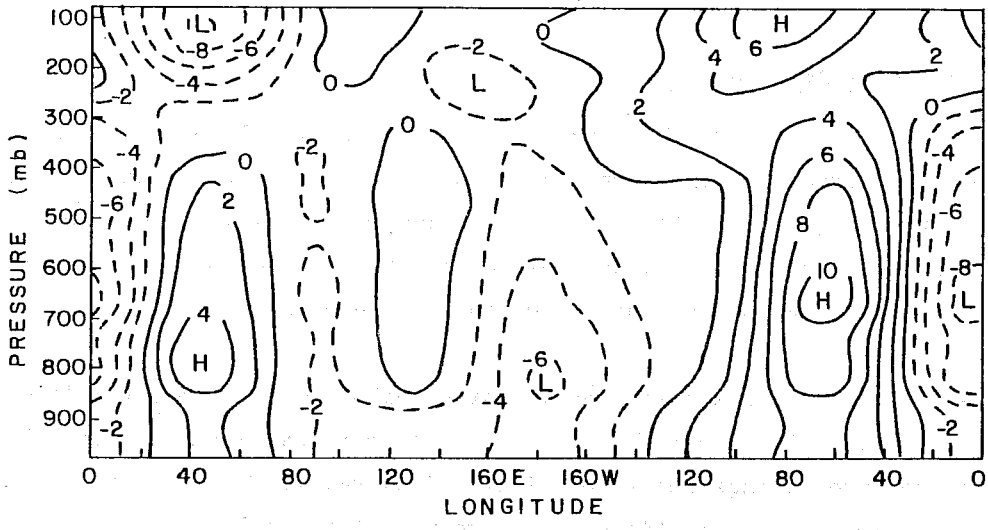

Fig. 11 Ensemble mean of the temperature forecast error at t = 10 days, 56° N, as a function of pressure and longitude, in °C. The dashed contours are negative.

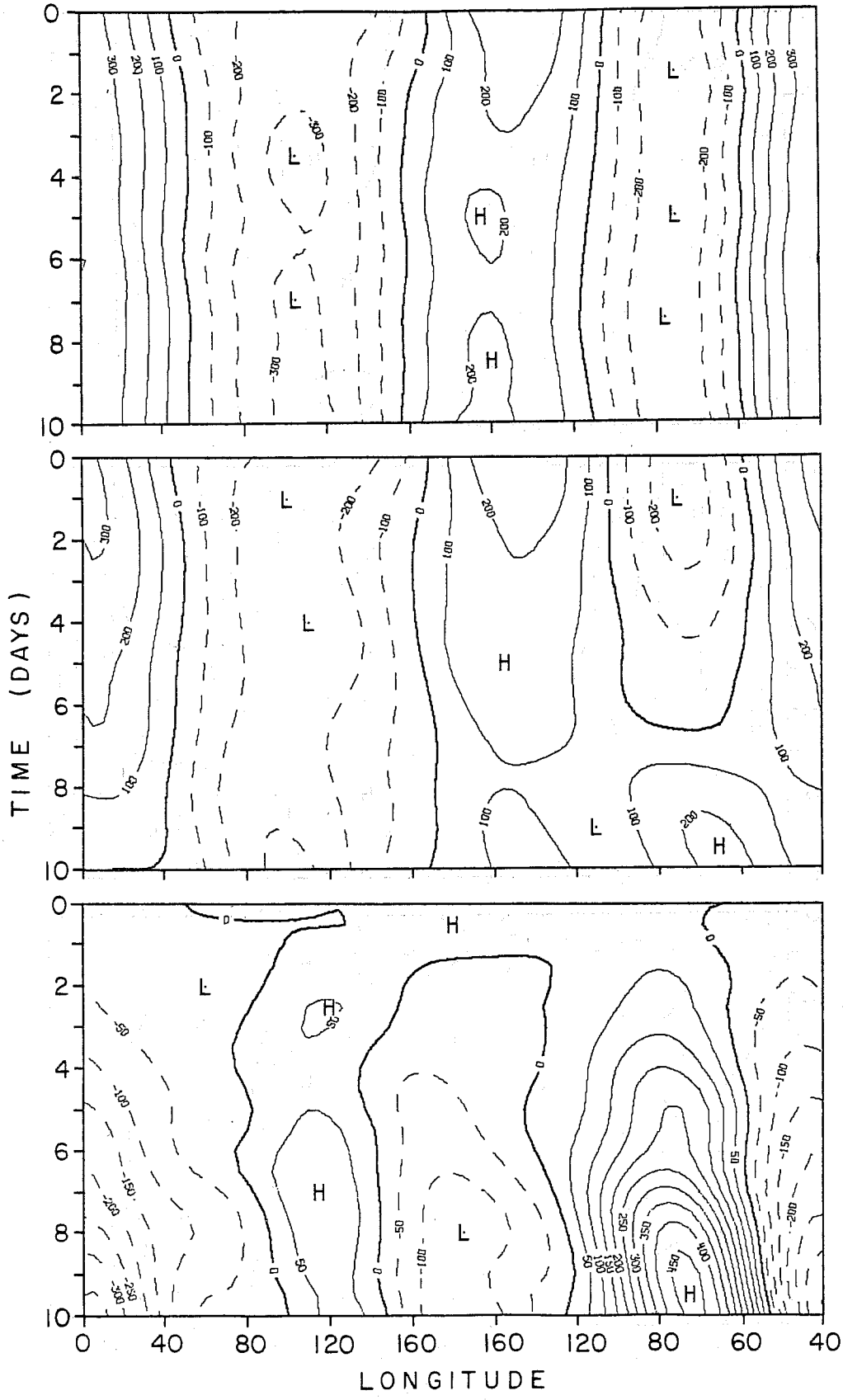

Fig. 12 Ensemble mean height field at 100 mb as a function of time and longitude at 56° N, including only zonal harmonics 1 to 4. Top: Analyses, contour interval 100 m. Centre: Forecasts, contour interval 100 m. Bottom: Forecast errors, contour interval 50 m. The dashed contours are negative.

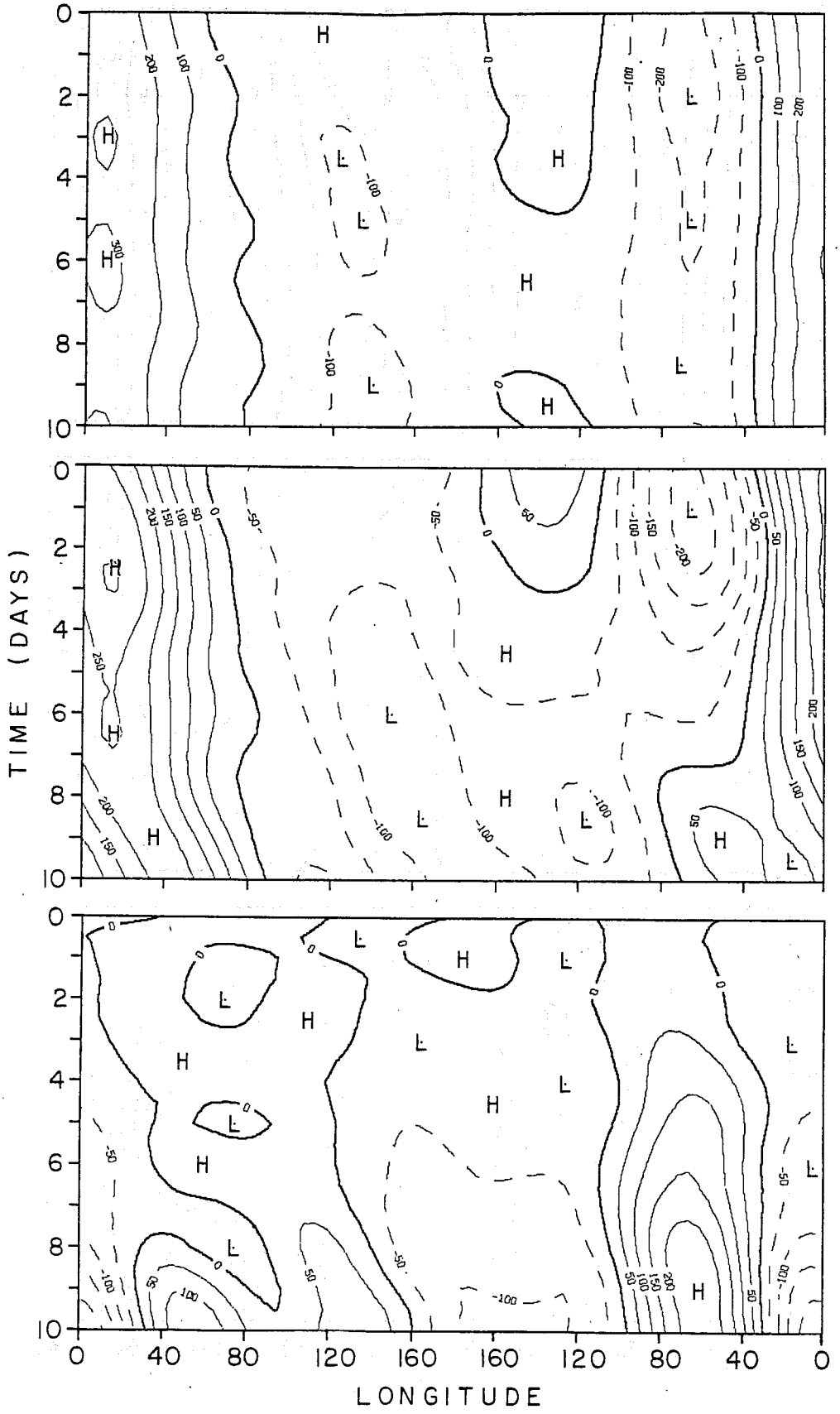

Fig. 13 As in Fig. 12 but at 500 mb.

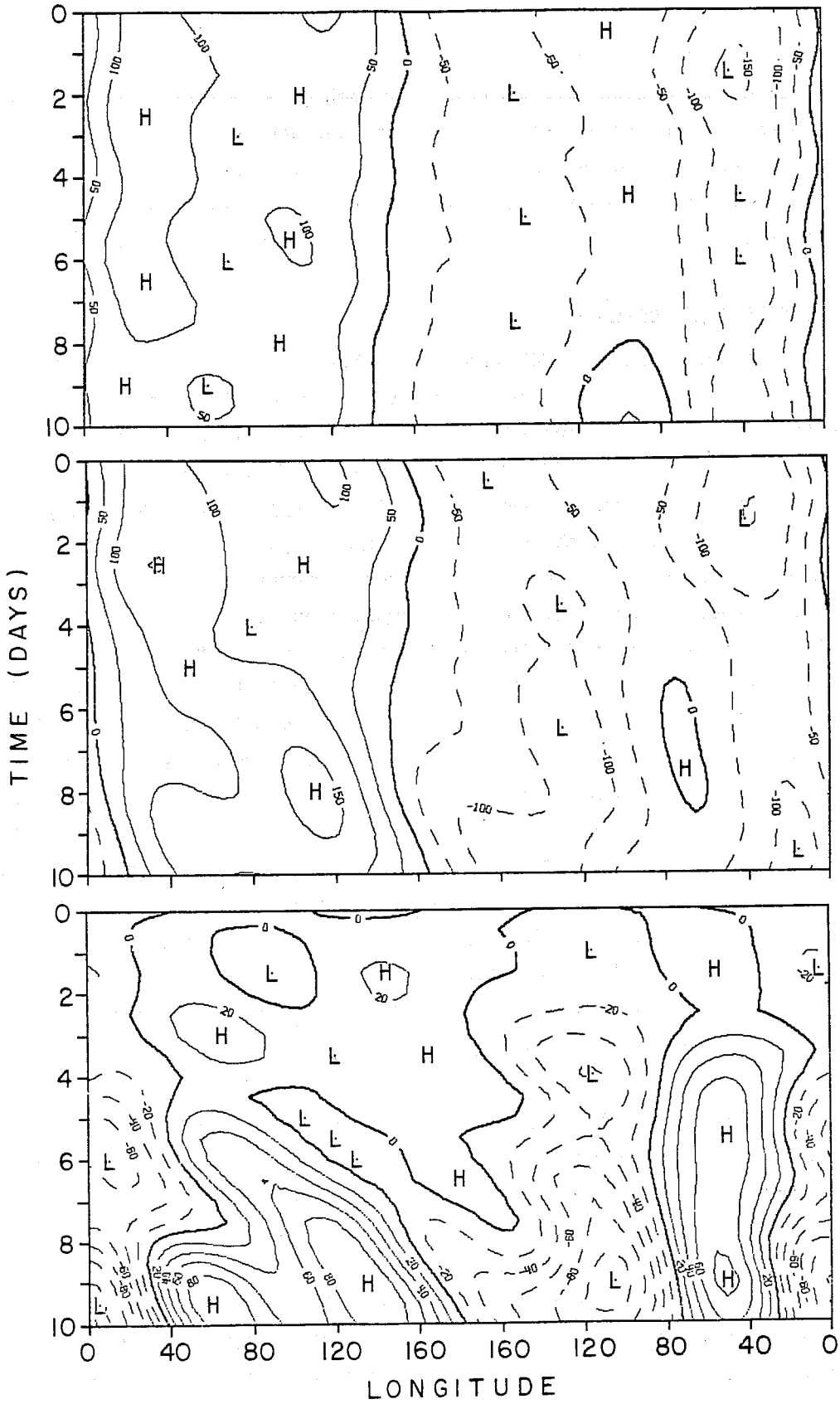

Fig. 14 As in Fig. 12 but at 1000 mb.

Hovemoller diagrams were also examined for each of harmonics 1 through 4 but the diagrams are not presented here. As the average analyses change relatively little with time and as the forecast harmonics change nearly linearly in time, the errors also change nearly linearly with time. The error Hovemoller diagrams then add relatively little to the information already contained in Fig. 6.

3.6 Vertical propagation

Bates (1977) and Laprise (1978) have shown that in a simplified, linearized model of the atmosphere the tropospheric structure of the forced planetary waves is sensitive to the specification of model conditions in the stratosphere. Similarly Lindzen et al (1968), Nakamura (1976) and Kirkwood and Derome (1977) have shown that in linearized β-plane models the upper boundary condition $\omega = dp/dt = 0$, where p is the pressure, causes a spurious wave energy reflection which can affect the tropospheric structure of vertically propagating planetary waves. Nakamura (1976) and Desmarais and Derome (1978) have then shown how this improper modelling of the stationary planetary waves can lead to forecast errors. It is clear that the models used in the above studies are highly simplified. For example, even in the most complex among them, that of Laprise (1978), the primitive equations in spherical geometry are used with a mean zonal wind varying both in pressure and latitude, but the equations are linearized and the forcing is very much simplified. It is therefore not evident to what extent the results of these studies are applicable to the fully non-linear numerical weather prediction models. It is quite possible that in the latter models the errors involved in the computation of the quasi-stationary energy sources and in the interactions between the transient and stationary waves far outweigh the effects of the reflective upper boundary condition or of the poor stratospheric resolution.

It does not appear possible, with the data of the present study, to determine the main cause of the average errors. For example, if the upper boundary condition or the poor stratospheric resolution were a significant source of error, one might hope to see the error first near the top of the model, and then observe in time its downward propagation to the lowest levels of the model. Matters are complicated, however, by the fact that, as Clark (1972) pointed out, quasi-geostrophic flow can propagate energy in the vertical with infinite speed. In other words, if an energy source is switched on, as in Clark's study, at the lower boundary of a quasi-geostrophic model at some time t the streamfunction tendency at that instant is non-zero at all points above the energy source and hence the source is felt throughout the fluid instantaneously. This effect is due at least in part to the hydrostatic approximation which forces the mass field to adjust instantaneously in a vertical column, and hence it should be

present to some extent in the ECMWF model. We can see that by considering the equation for the surface pressure tendency in sigma coordinates,

$$\partial p_s/\partial t = - \nabla \cdot (\bar{\underset{\sim}{V}} p_s)$$

where $\bar{\underset{\sim}{V}}$ is the vertically averaged horizontal wind vector. Thus if $\underset{\sim}{V}$ is changed at any point in a vertical column the surface pressure tendency is affected instantaneously.

In spite of the above difficulty we decided to examine the time evolution of the average forecast height error to see whether or not any vertical propagation could be detected. This was done by first computing the root mean square error along 56° N at each pressure level from t = 0 to t = 10 days at 12-hour intervals. The results are shown in Fig. 15(a). Here zonal harmonics 1 through 20 have been included and the results were filtered in time with weights 0.25, 0.50, 0.25. We see that the time evolution of the error takes the appearance of a steady growth at all levels on which are superimposed shorter time scale bursts of more rapid or slower growth. To see more clearly these shorter time scale fluctuations we computed the time derivative of the error in Fig. 15(a) by means of 12 hour time differences; the result is the "error growth per 12 hours" shown in Fig. 15(b). We note first that the time scale of these fluctuations is comparable with that of the analyses as revealed by the Hovemoller diagrams of Fig. 12, 13, 14. In other words, the time fluctuations seen in Fig. 15(b) may well be a reflection of our small sample and should therefore not be associated with the systematic errors of the model. Nevertheless, even though the fluctuations can be the result of a single forecast contributing strongly to the error, they are of interest in that they provide information on the rate at which the error growth can propagate vertically in a given forecast. For example, the ridge line which extends from p = 250 mb at t = $1^3/_4$ days to 1000 mb at t = 3 days is suggestive of a descent in time of the error growth. Similarly the large error growth which reaches a maximum at the top level at t = 7 days appears to propagate rather quickly downward.

Similar diagrams were constructed for the contributions by the separate harmonics m = 1 to 4. The diagrams for m = 1 and 2 are shown in Figs. 16 and 17 respectively. Those for m = 3 and 4 did not show any vertical propagation and are not reproduced here. For m = 1 the error has relatively little vertical structure in the initial stages of the forecasts but with time we see that the error becomes concentrated in the upper half of the domain. Turning to the error growth in Fig. 16(b) we find a ridge pattern originating at 1000 mb at t = $2^1/_4$ days and sloping upwards with time to approximately 150 mb

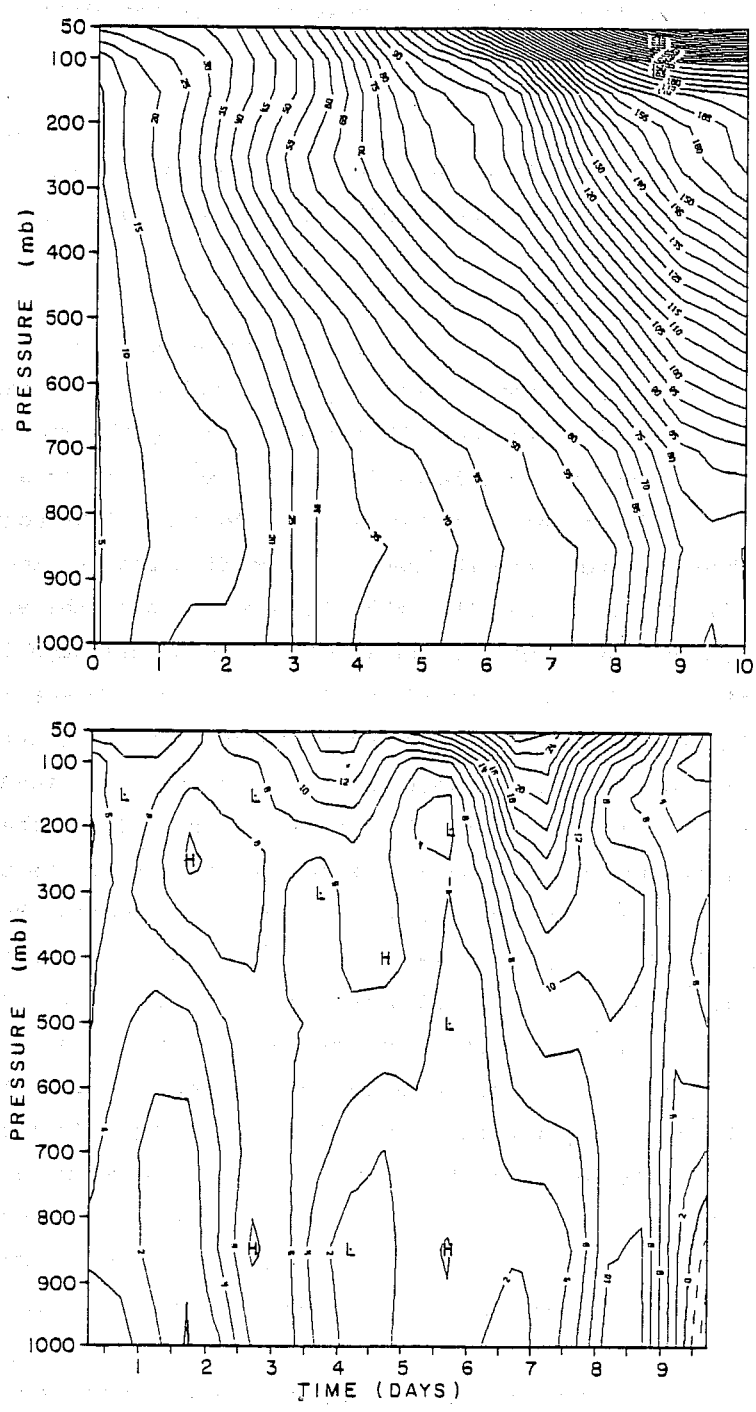

Fig. 15 (a) The ensemble mean height forecast error averaged in a rms sense along 56° N, as a function of pressure and time. Zonal harmonics m = 1 to 20 have been included. The contour interval is 5 m. (b) The time tendency of the height forecast error obtained by taking 12-hour differences of the data in (a). The units are m/(12 hours) and the contour interval is 2 units.

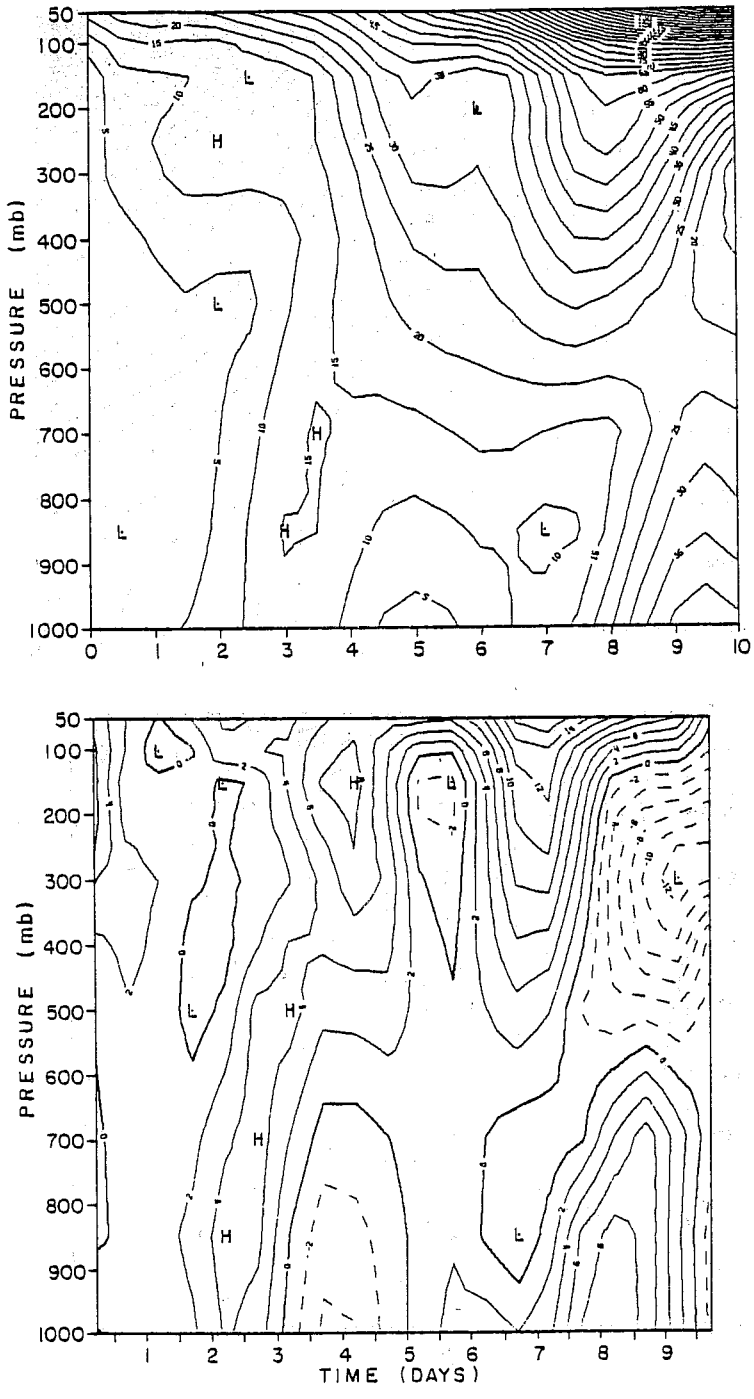

Fig. 16 As Fig. 15 but for zonal harmonic m = 1.

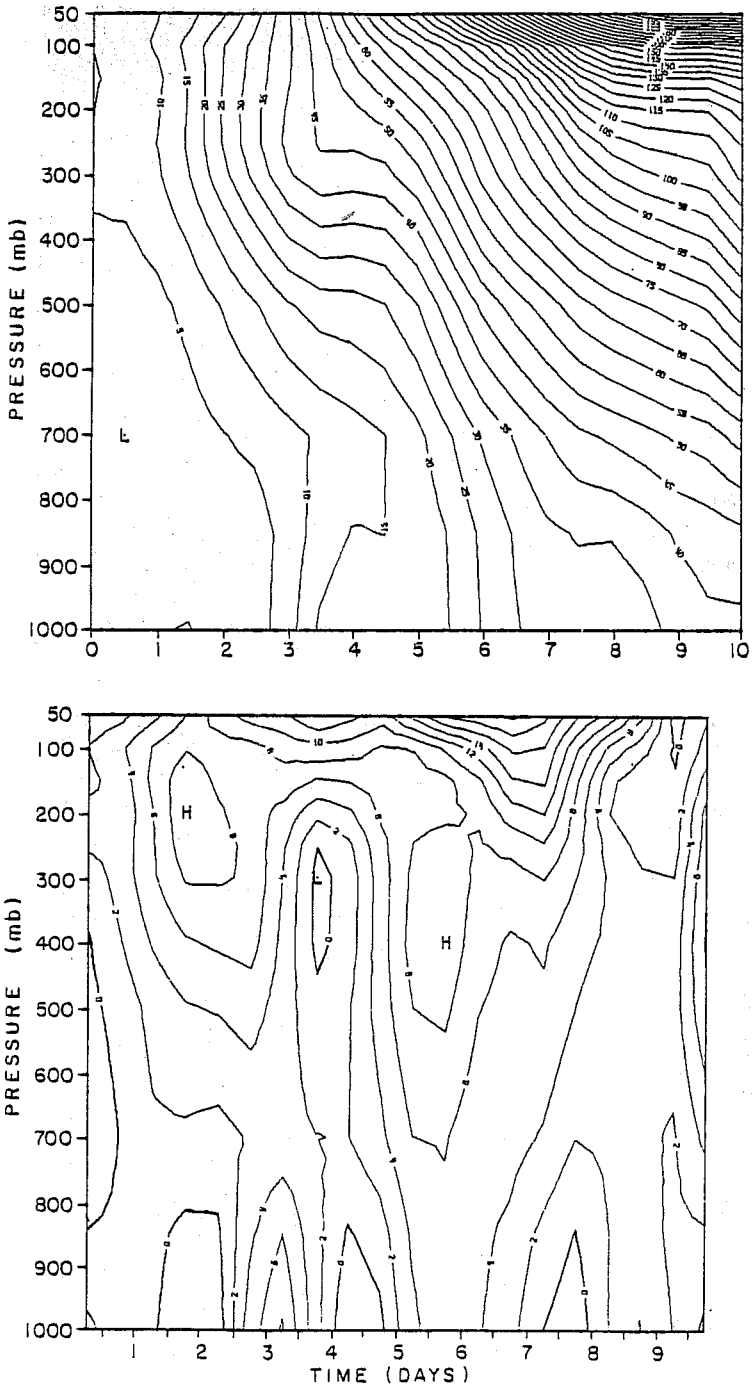

Fig. 17 As Fig. 15 but for zonal harmonic m = 2.

at $4^1/_4$ days indicating an upward propagation of the error in wave number one. In addition there is a secondary ridge line extending downwards with time from approximately 150 mb at $4^1/_4$ days suggesting a downward propagation of the error, perhaps as a result of a reflection of the upward propagating pulse. It should be noted that the features just described take place over several time levels of data so that the slopes that are depicted are probably not strongly affected by the sampling frequency. There are other features in the figure, however, which are nearly vertical, such as the ridge in the upper half of the domain near t = 7 days. As they involve fewer time levels they are more likely to have been affected by the 12 hour sampling time and our time filter. We will therefore not discuss them further.

The corresponding diagrams for zonal wave number 2 (Fig. 17) show naturally some similarities with those of Fig. 15 as m = 2 is the dominant contributor to the geopotential height error. We note, in particular, the suggestion of a downward propagation of the error growth from approximately p = 200 mb, t = $1^3/_4$ days, as already discussed in the context of the total error growth in Fig. 15(b).

So we have seen in this section that part of the error takes the form of pulses which propagate vertically, superimposed on a much more important monotonic growth. The pulses are believed to result from our small sample and are probably not associated with any systematic error of the model. They are, however, interesting in that they give us some idea of the rate at which information can propagate vertically in the model on the scale of planetary waves.

The data we have presented in this section have not shown whether or not the reflective upper boundary condition and the limited stratospheric vertical resolution have a significant influence on the systematic errors of the model. They seem to indicate, however, that events taking place at the upper levels of the model can propagate their influence to the middle troposphere in a matter or a day or two.

4. SUMMARY OF RESULTS AND DISCUSSION

The dominant features of the average forecast errors that we have examined take the form of excessively low pressure patterns centered approximately over Great Britain and in the Gulf of Alaska at all levels. There seems to be no significant meridional propagation of the errors throughout the forecast period, but some eastward propagation, particularly at 500 mb. This is associated with the tendency of the model to shift the European ridge at that level eastward while the Atlantic low in the model gradually fills, in fact becoming a ridge at t = 10 days, the latter effect being quite pronounced at both 500 mb and 100 mb. Although some vertical propagation of the error has been observed, it is not believed to be related to a systematic deficiency of the model but rather to a contribution by one, or a few, of the cases in our sample.

A Fourier analysis of the geopotential height data at 100, 500 and 1000 mb at 56^{o} N, where the error is largest, has shown that the main deficiency of the model is its inability to maintain the amplitude of zonal wave number m = 2 in the middle and upper troposphere. The forecast and observed harmonics m = 2 do not bear a constant phase relationship to each other but the forecast error wave is very nearly vertical. Although the height error spectrum is dominated by zonal wave number 2 at 500 mb, the normalized spectrum, obtained by dividing the error amplitudes by the observed ones, shows no peak at m = 2.

Unfortunately it does not appear possible with the data of the present study to determine the main cause, or causes, of the average forecast errors. Some similarities have been noted between the spatial distributions of the errors at t = 10 days and t = 0, that is, immediately after the nonlinear normal mode initialization done with the adiabatic equations but the long-term integration described by Arpe (1980) suggests that the source of the errors does not lie in the initial conditions of the model.

While it is necessary to study and describe the structure of the systematic errors of numerical models, it is to be expected that the main causes of errors is more likely to be found by performing forecast sensitivity experiments in which some aspects of the model are modified in a systematic manner. It must be kept in mind, however, that there are several features of the model to be examined, for example, the parameterization of sub-grid scale processes with its many components, so that a satisfactory solution to the problem may require a considerable effort.

REFERENCES

Arpe, K., 1980 Preliminary assessment of a 50 day run with the ECMWF operational forecast model. ECMWF Technical Memorandum No.12, pp.36. Available from ECMWF library.

Bates, R., 1977 Dynamics of stationary ultra-long waves in the middle latitudes. Quart. J. Roy. Meteor. Soc., 103, 397-430.

Clark, J.H.E., 1972 The vertical propagation of forced atmospheric planetary waves. J. Atmos. Sci., 29, 1430-1451.

Desmarais, J.-G. and J. Derome, 1978 Some effects of vertical resolution on modelling forced planetary waves with a time-dependent model. Atmosphere-Ocean, 16, 212-225.

Hollingsworth, A., K. Arpe, M. Tiedtke, M. Capaldo and H. Savijärvi, 1980 The performance of a medium range forecast model in winter - Impact of physical parameterizations. Mon. Wea. Rev., 198, 1736-1773.

Hoskins, B.J. and D.J. Karoly, 1980 The steady linear response of a spherical atmosphere to thermal and orographic forcing. Submitted to J. Atmos. Sci.

Kirkwood, E. and J. Derome, 1977 Some effects of the upper boundary condition and vertical resolution on modelling forced stationary planetary waves. Mon. Wea. Rev., 105, 1239-1251.

Laprise, R., 1978 On the influence of stratospheric conditions on forced tropospheric waves in a steady-state primitive equation model. Atmosphere-Ocean, 16, 300-314.

Lindzen, R.S., E.S. Batten and J.W. Kim, 1968. Oscillations in atmospheres with tops. Mon. Wea. Rev., 96, 133-140.

Nakamura, H., 1976 Some problems in reproducing planetary waves by numerical models of the atmosphere. J. Meteor. Soc. Japan, 54, 129-146.

Tiedtke, M., J.-F. Geleyn, A. Hollingsworth and J.-F. Louis, 1979 Parameterization of subgridscale processes. ECMWF Technical Report No.10, pp.46.

ECMWF PUBLISHED TECHNICAL REPORTS

No. 1 A Case Study of a Ten Day Prediction

No. 2 The Effect of Arithmetic Precisions on some Meteorological Integrations

No. 3 Mixed-Radix Fast Fourier Transforms without Reordering

No. 4 A Model for Medium-Range Weather Forecasting - Adiabatic Formulation

No. 5 A Study of some Parameterizations of Sub-Grid Processes in a Baroclinic Wave in a Two-Dimensional Model

No. 6 The ECMWF Analysis and Data Assimilation Scheme - Analysis of Mass and Wind Fields

No. 7 A Ten Day High Resolution Non-Adiabatic Spectral Integration: A Comparative Study

No. 8 On the Asymptotic Behaviour of Simple Stochastic-Dynamic Systems

No. 9 On Balance Requirements as Initial Conditions

No.10 ECMWF Model - Parameterization of Sub-Grid Processes

No.11 Normal Mode Initialization for a multi-level Gridpoint Model

No.12 Data Assimilation Experiments

No.13 Comparison of Medium Range Forecasts made with two Parameterization Schemes

No.14 On Initial Conditions for Non-Hydrostatic Models

No.15 Adiabatic Formulation and Organization of ECMWF's Spectral Model

No.16 Model Studies of a Developing Boundary Layer over the Ocean

No.17 The Response of a Global Barotropic Model to Forcing by Large-Scale Orography

No.18 Confidence Limits for Verification and Energetics Studies

No.19 A Low Order Barotropic Model on the Sphere with the Orographic and Newtonian Forcing

No.20 A Review of the Normal Mode Initialization Method

No.21 The Adjoint Equation Technique Applied to Meteorological Problems

No.22 The Use of Empirical Methods for Mesoscale Pressure Forecasts

No.23 Comparison of Medium Range Forecasts made with Models using Spectral or Finite Difference Techniques in the Horizontal

No.24 On the Average Errors of an Ensemble of Forecasts